Computer simulation of atomic-displacement cascades in solids in the binary-collision approximation

Mark T. Robinson*

Solid State Division, Oak Ridge National Laboratory, Oak Ridge, Tennessee 37830

Ian M. Torrens†

Centre d'Etudes Nucléaires de Saclay, France
(Received 12 November 1973)

A comprehensive computer program has been developed for the simulation of atomic-displacement cascades in a variety of crystalline solids, using the binary-collision approximation to contruct the projectile trajectories. The atomic scattering is governed by the Moliére potential. Impact-parameter-dependent inelastic losses are included using Firsov's theory. Thermal vibrations of the target atoms and crystal surfaces may be included. Permanent displacement of lattice atoms may be based on either an energy-threshold criterion or a Frenkel-pair-separation criterion. An extensive series of calculations has been made for cascades in the simple metals Cu, Fe, and Au, to test the effects on the results of many of the model parameters. When a displacement-threshold energy is used, the number of Frenkel pairs is found to be a linear function of that part of the primary recoil energy which remains as the kinetic energy of atoms. This result is independent of target temperature, of the presence or absence of inelastic energy losses, and of various details of the model. In contrast, when a separation criterion is used, the number of defects increases less rapidly than linearly. This effect is caused by increased recombination in the highly disturbed tracks of the energetic recoils. Agreement between theoretical and experimental estimates of the radiation damage produced by neutron irradiation of Cu is substantially improved in the latter model.

I. INTRODUCTION

The theoretical understanding of atomic-displacement effects in solids requires a detailed analysis of the dependence of the number of point defects produced and their spatial distribution on the energy of the primary recoil atoms. These atoms, originally set into motion by interactions with incident electrons, neutrons, or ions, dissipate their initial kinetic energies in a series of inelastic encounters with other atoms of the solid, displacing some of these to slow down in their turn by a similar series of collisions. The resulting cascade of displaced atoms and their accompanying vacancies are eventually responsible for the changes which occur in the irradiated solid. These may include erosion of the target (sputtering) or alterations in its physical properties (radiation damage) or chemical composition (hot-atom chemistry). The theory of the displacement cascade is thus of interest in several related fields, some of which are of technological importance. Analytical treatments of this theory have been reviewed recently.[1,2] These generally involve more-or-less severe approximation of the problem, such as ignoring the crystal structure of the target and the loss of energy by electron excitation or restricting the treatment to hard-core scattering or other simplified atomic-scattering laws. The object of the present work was to develop a comprehensive computational model, including as many aspects of the physical situation as possible, which would allow a fairly realistic computer simulation of displacement-cascade production in crystalline solids. In this communication, the model is described in detail and an application is given to radiation damage in pure metals. A preliminary account of some of this work has appeared previously.[3] Applications of the program to sputtering[4] and to a problem in hot-atom chemistry[5] are presented elsewhere.

Computer-simulation techniques were first introduced into studies of low-energy radiation-damage events by Vineyard et al.[6-8] They studied small crystallites of a few hundred atoms, with boundary restraints chosen to represent imbedding in a larger matrix. Some kinetic energy was given to one atom and the classical equations of motion of the mutually interacting atoms of the numerical crystallite were integrated until this energy was dissipated. Such calculations are particularly useful in studying the geometry, stability, and motion of point defects, the threshold energy for producing stable defects, and radiation damage events at primary recoil energies below about 1 keV. The method gives considerable insight into the dynamics of radiation damage in the domain where it is applicable. It has been applied to alkali halides,[9] to bcc metals,[7,8] and to fcc metals.[6,10] Without the boundary restraints, the technique has also been applied to studies of sputtering.[11] The required crystallite sizes and computation times probably preclude its extension to the high energies characteristic of fast-neutron damage in reactor materials. It is also generally restricted to stud-

ies where statistical information is unnecessary. An alternative procedure, followed in the present work, is to construct the trajectory of a moving particle as a series of isolated binary collisions, an approximation which is especially useful at high energies where collision times are very short. This technique.has been used previously in radiation-damage calculations by Beeler.[12-16] It has also been used in studies of the ranges of energetic atoms in solids[17-19] and in studies of channeling.[18, 20-22] It can be made sufficiently fast to allow studies of ensembles of primaries to be performed and the inclusion of many high-energy features such as energy loss by electron excitation is straightforward. On the other hand, especially at low energies, isolation of the collisions is difficult and various *ad hoc* features must be added to the model to simulate many-body effects. These points will be considered more fully as the details of the model are presented.

The model is based on a recognition that the various steps in producing radiation effects in solids proceed on rather disparate time scales and may, therefore, be separated. The nuclear events involved in producing the primary recoils are very fast. Even the lifetimes of compound nuclei are generally short enough to be ignored. Recent measurements[23] have shown the lifetimes of excited compound nuclei in the $Ge(p, p')$ reaction to lie in the $(3-6) \times 10^{-17}$-sec region. In such times, even MeV recoils move less than about 1 Å. Thus, the primary recoils may usually be regarded as stable and proceeding directly from the site of the inciting nuclear encounter. At the other extreme, the characteristic thermal-vibration periods of atoms in solids lie in the region of 10^{-13} sec or longer. This time is sufficient for the thermal displacements of atoms in a crystal to be regarded as frozen during the development of a single displacement cascade. Eventually, as the particles slow down, they will reach an energy at which they no longer collide with individual atoms of the medium, but instead interact with the crystal as a whole. One estimate of the energy at which such many-body effects might supervene can be made by equating the velocity of the moving atom to the velocity of longitudinal (sound) waves in the solid. Below this critical energy, strong many-body effects, analogous perhaps to the Mössbauer effect, may be anticipated. The critical energies for a number of metals are listed in Table I. These provide a partial statement of the lower limit of validity of the binary-collision approximation. This will be amplified in a later section.

In brief outline, the computer program starts with a primary recoil of specified energy, position, and direction. This is followed through a series of inelastic binary atomic collisions. If the energies

TABLE I. Critical energies for strong many-body effects on displacement-cascade development.

Metal	Longitudinal wave velocity $(10^{13}$ Å/sec)[a]	Single atom energy (eV)
Al	6.26	5.48
Cu	4.70	7.27
Pt	3.96	15.9
Au	3.24	10.7
Fe	5.85	9.90
W	5.46	28.4

[a]C. Kittel, *Introduction to Solid State Physics* (Wiley, New York, 1953), p. 57.

which they receive are sufficiently great, the target atoms in these collisions will be added to the cascade. To simulate the development of the cascade in time, the program always follows the current fastest particle. When the energy of a particle becomes sufficiently small, when it escapes from the target, or when it meets certain other preassigned conditions, it is dropped from the cascade. When no particles remain to be followed, various analyses of the results of the calculation are performed. The details of the calculation are presented in the following sections. These discuss respectively the treatment of the individual binary collisions, the selection of suitable interatomic potential and inelastic-energy-loss functions, the description of the crystal and the development of a cascade, and the atomic displacement process. This is followed by a discussion of some limitations of the binary-collision approximation. The use of the program is then illustrated by some calculations for pure metals, with particular emphasis on understanding the response of the model to alterations in its various parameters. Comparisons are made with previous machine calculations[12-16] and with analytical cascade theories. The program has been named MARLOWE. This name will be used occasionally as a convenient shorthand.

II. TREATMENT OF BINARY COLLISIONS

It is assumed in the computational model that the particles move only along straight-line segments, these being the asymptotes of their paths in the laboratory (L) system. The inelastic atomic collisions are considered to be composed of a quasielastic part and of an essentially separate electron excitation part. This separation is permissible partly because the low mass of electrons prevents them from carrying significant momentum and partly because the inelastic energy loss in individual collisions is small. The quasielastic atomic scattering is described with sufficient accuracy by classical mechanics. The conditions for the validity of

this assumption are discussed elsewhere.[1,2,24,25]
The trajectories of two particles interacting according to a conservative central repulsive force are shown in Fig. 1, which defines several terms of interest. The equations of motion which describe these trajectories can be manipulated in the usual manner[26,27] to yield the barycentric scattering angle

$$\theta = \pi - 2s \int_R^\infty dr [r^2 g(r)]^{-1} \qquad (1)$$

and time integral

$$\tau = (R^2 - s^2)^{1/2} - \int_R^\infty dr \left[[g(r)]^{-1} - \left(1 - \frac{s^2}{r^2}\right)^{-1/2} \right], \quad (2)$$

where

$$g(r) = [1 - s^2/r^2 - V(r)/E_r]^{1/2}, \qquad (3)$$

s is the impact parameter, E_r is the relative kinetic energy, r is the (variable) interatomic separation, $V(r)$ is the potential of interatomic force, and R is the apsis of the collision defined by $g(R) = 0$. The relative kinetic energy is

$$E_r = A E_0/(1+A), \qquad (4)$$

where E_0 is the incident kinetic energy of the projectile and A is the ratio of the mass of the target (scattering) atom to that of the projectile (scattered) atom. The integrals in Eqs. (1) and (2) are evaluated by four-point Gauss-Mehler quadrature.[28,29]

The conversion of the barycentric quantities to the L system follows standard procedures.[26,27] The L scattering angles of the projectile and the target are

$$\tan\vartheta = Af\sin\theta/(1 + Af\cos\theta), \qquad (5)$$

$$\tan\phi = f\sin\theta/(1 - f\cos\theta), \qquad (6)$$

where

$$f = (1 - Q/E_r)^{1/2} \qquad (7)$$

and Q is the energy lost by electron excitation. The energy transferred to the target atom in the collision is

$$T = [f \sin^2 \tfrac{1}{2}\theta + \tfrac{1}{4}(1-f)^2] T_m , \qquad (8)$$

where the maximum transferred energy is

$$T_m = 4 E_r/(1+A). \qquad (9)$$

The energy of the projectile after scattering is

$$E_1 = E_0 - T - Q. \qquad (10)$$

Location of the asymptotic L trajectories requires the evaluation of the quantities x_1 and x_2 in Fig. 1. To do this, imagine that the collision begins with the projectile at a distance r from the target sufficiently great that its deviation from the incoming asymptote can be neglected. The barycenter moves at constant velocity along the line $y = s/(1+A)$. When the particles reach the apsis of the collision, the barycenter has moved to the right from its original position a distance

$$x_0 = [(r^2 - s^2)^{1/2} - \tau]/(1+A).$$

It continues its rectilinear motion until the collision partners have again receded to a distance r from one another, now on their outgoing asymptotes. The barycenter has moved an additional amount x_0/f. Since the relative kinetic energy has been reduced by the inelastic loss, the final relative velocity of the two particles is reduced by a factor
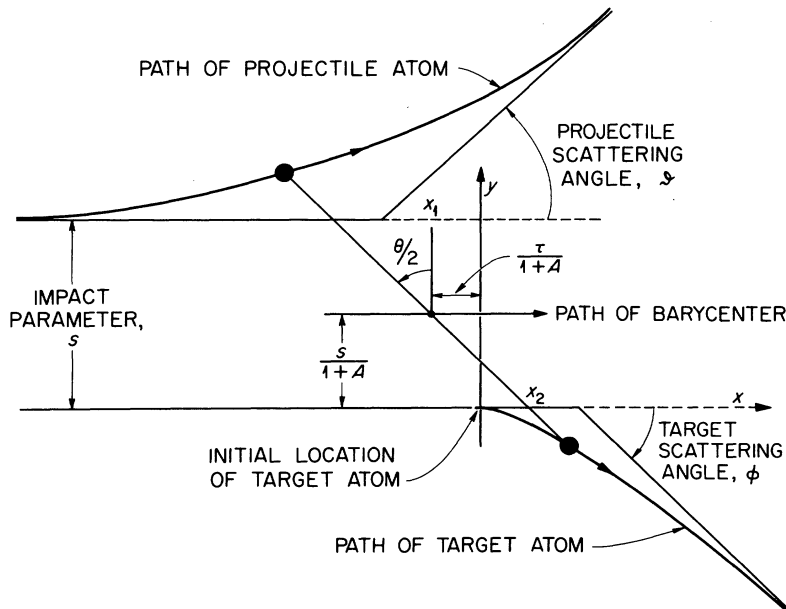

PATH OF PROJECTILE ATOM

PROJECTILE SCATTERING ANGLE, ϑ

x_1

$\theta/2$

$\frac{\tau}{1+A}$

IMPACT PARAMETER, s

$\frac{s}{1+A}$

PATH OF BARYCENTER

x_2

x

INITIAL LOCATION OF TARGET ATOM

TARGET SCATTERING ANGLE, ϕ

PATH OF TARGET ATOM

FIG. 1. L trajectories of two particles interacting according to a conservative central repulsive force. The positions of the particles and of the barycenter are shown at the apsis of the collision.

f. Hence, the barycenter moves farther in the second part of the collision than in the first. The angle between the barycentric velocity and the radius vector connecting the particles is now

$$\theta + \sin^{-1} s/r.$$

It is a simple matter to locate the two particles in the laboratory and to evaluate the intersections of the incoming and outgoing asymptotes. The results are

$$x_1 = [(1+f)\tau + (fA - 1) \, s \, \tan\tfrac{1}{2}\theta]/f(1+A), \qquad (11)$$

$$x_2 = s \, \tan\tfrac{1}{2}\theta - x_1 . \qquad (12)$$

In MARLOWE, the particles move along straight-line segments from one laboratory deflection point to the next. Note that although the inelastic energy loss does not enter the barycentric equations of motion, it does affect the kinematics of the collision through Eq. (7). The program contains three options with respect to the inelastic losses. These may be omitted altogether ($Q \equiv 0$ and $f \equiv 1$), they may be included in the energy loss, but omitted from the kinematics ($Q \neq 0$, but $f \equiv 1$), or they may be included as described. The nonzero value of x_2 simulates the fact, easily seen in dynamic programs,[6-10] that targets begin to move before the deflection of the projectile. The program allows the option of ignoring this, that is, of taking $x_2 \equiv 0$. It also allows the option of taking $\tau \equiv 0$. This group of options is included to permit tests of the importance of various details of the treatment of binary collisions on the overall results of the calculation.

The treatment of the individual collisions adopted here differs from Beeler's[12] in two respects. First, his program included no inelastic energy losses. Second, his procedure for locating the particle trajectories in space corresponds to approximating the time integral by its hard-core value $s \tan\tfrac{1}{2}\theta$. This makes $x_2 = 0$ and results in targets moving directly off their lattice sites. The effects of these two differences between the models have been studied extensively and will be discussed below.

III. INTERATOMIC POTENTIAL AND INELASTIC ENERGY LOSS

The difficult general problem of selecting an interatomic potential function for various applications is discussed elsewhere.[1,30,31] In the present application, the distances between the interacting atoms may vary from very small values (< 0.1 Å) at the apsides of high-energy head-on collisions to something more than half the nearest-neighbor distance in the target crystal. Proper treatment of the high-energy region dictates the use of a screened Coulomb potential

$$V(r) = (Z_1 Z_2 \, e^2/r) \, \Phi(r/a_{12}), \qquad (13)$$

where $Z_1 e$ and $Z_2 e$ are the nuclear charges of the projectile and target, respectively, $\Phi(x)$ is a suitable screening function, and a_{12} is a screening length which depends on the properties of the collision partners. While MARLOWE is constructed to allow fairly easy alteration of the potential function, all calculations to date have used the Molière approximation[32] to the Thomas-Fermi screening function

$$\phi(x) = 0.35 y + 0.55 y^4 + 0.10 y^{20}, \qquad (14)$$

where

$$y = e^{-0.3x}.$$

This function represents the Thomas-Fermi atomic screening function quite accurately for $x < 5$; for larger separations it decreases exponentially, rather than as x^{-3}. The use of Eq. (14) is partly a matter of convenience, but recent experiments on planar channeling have been interpreted in terms of closely similar functions.[33]

The choice of screening lengths in the calculation may be made in either of two ways. Firsov,[34] on the basis of approximate numerical solutions of the Thomas-Fermi diatomic molecule problem, has suggested the formula

$$a_{12} = (\tfrac{9}{128} \pi^2)^{1/3} a_B (Z_1^{1/2} + Z_2^{1/2})^{-2/3}, \qquad (15)$$

where a_B is the Bohr radius. This screening length is optionally available in the program. It is also possible to use screening lengths deduced in other ways. In most of the present work, the screening lengths have been estimated by matching the Molière potential at the nearest-neighbor distance to a Born-Mayer potential whose parameters were obtained mainly from equilibrium crystal data. These estimates are compared with the Firsov parameters in Table II. Figure 2 compares some screening functions for Cu-Cu interactions. The Born-Mayer potentials used in the matching procedure were those of Vineyard *et al.*, for Cu (Ref. 6) and Fe (Ref. 7) and that of Thompson for Au.[35] These potentials were also used by Beeler in his machine calculations.[12-16]

Inelastic energy losses are included in the program using a modification of a model proposed by Firsov.[36] In this model, the origin of the inelastic energy loss was found in the momentum possessed by the electrons of the projectile because of its motion in the L system. The collision time was regarded as sufficiently long that the electrons of the two colliding systems were completely mixed and the inelastic energy loss was calculated from the momentum transfer in this mixing process. The nuclear motion was described by the impulse approximation and an approximate Thomas-Fermi description of the two atoms was used. This theory has been modified here by using the apsis of

TABLE II. Screening lengths based on matching the Molière and Born-Mayer potentials compared with the values of Firsov.

	Screening lengths (Å)		Nearest-neighbor distance (Å)
	Firsov	Matching	
Cu	0.0960	0.0738	2.556
Fe	0.0996	0.0781	2.482
Au	0.0688	0.0752	2.884

the collision instead of the impact parameter, this change being regarded as a correction to the impulse approximation. The inelastic loss in a single collision is then

$$Q(s, E_0) = \alpha_{12} E_0^{1/2}/[1 + \beta_{12} R(s, E_0)]^5, \qquad (16)$$

where

$$\alpha_{12} = 0.61 \frac{2\hbar}{\pi a_B} \left(\frac{2}{m_1}\right)^{1/2} (\tfrac{9}{128}\pi^2)^{1/3} (Z_1 + Z_2)^{5/3}, \qquad (17)$$

$$\beta_{12} = (0.285/2a_B)(128/9\pi^2)^{1/3} (Z_1 + Z_2)^{1/3}, \qquad (18)$$

and m_1 is the mass of the projectile. The leading numerical factors in Eqs. (17) and (18) derive from an approximate numerical integration performed by Firsov.[36] The upper limit of validity of Eq. (16) does not exceed[37] $(\tfrac{1}{2}m_1) v_B^2 Z_1^{4/3}$, where $v_B = e^2/\hbar$. The model is thus not applicable to light projectiles at high energies. Our modification to Eq. (16) reduces the inelastic losses below the predictions of Firsov,[36] especially at low energies and small im-

pact parameters, and also alters the energy dependence. This is easily seen in Fig. 3, which compares the electronic stopping cross sections

$$S_e(E) = 2\pi \int_0^\infty s \, Q(s, E) \, ds \qquad (19)$$

for Cu recoils in Cu according to the present model, the original Firsov model, and the widely used stopping theory of Lindhard et al.[37] One point (the only one within the range of the figure) is also shown from the semiempirical correlation of Northcliffe and Schilling.[38]

IV. CRYSTAL DESCRIPTION AND CASCADE DEVELOPMENT

A principal advantage of the binary collision approximation is that it requires only a small amount of information to describe the target crystal. The scheme used in MARLOWE is a slight modification of an earlier one[17] which makes use of the translational symmetry of the crystal. A list is made of the positions of several atoms in the crystal, using one of the lattice sites as the origin of coordinates. The necessary atomic positions anywhere in the crystal may then be generated at will by using this list in conjunction with the position of a lattice site close to any moving cascade atom. The scheme permits the sites to be of different chemical or crystallographic type. As presently written, MARLOWE requires only that the crystal be describable by Cartesian (orthorhombic) coordinates; various copies of the program have allowed from two to ten types of atom and site in order to deal with
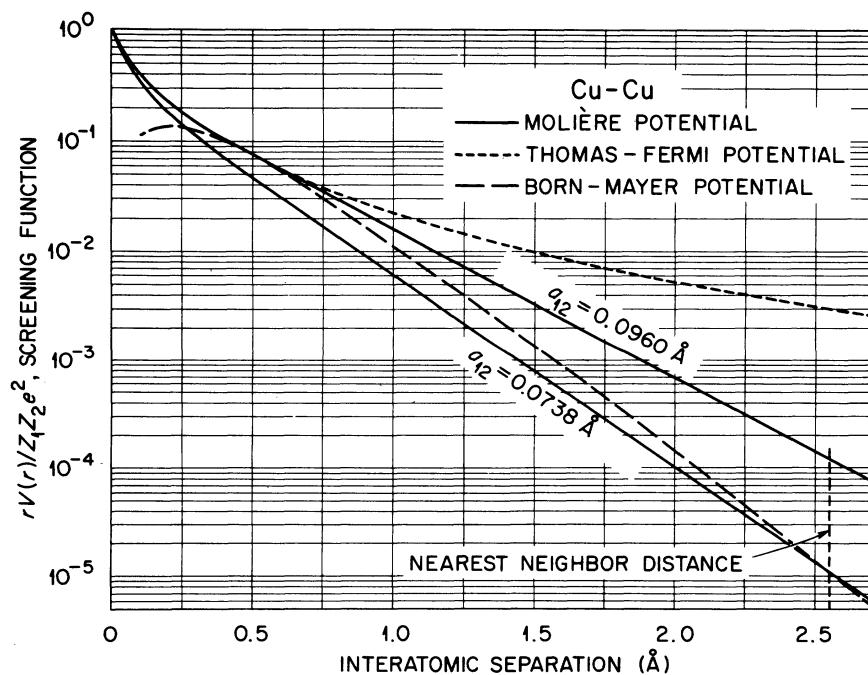

FIG. 2. Comparison of some screening functions for Cu–Cu interactions.
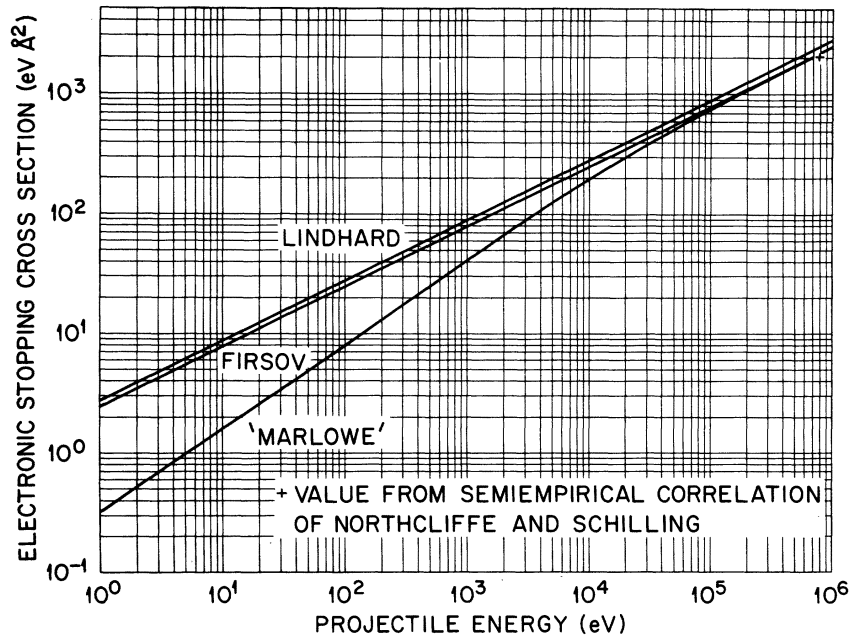
FIG. 3. Electronic stopping cross sections for Cu recoils in Cu in different approximations.

particular problems. Extension of the procedure to crystals of lower symmetry is straightforward, but substantial additional complexity would be introduced into the program, resulting in large increases in computing time. The number of atoms in the neighbor list is a compromise between the time required to search it and the probability of success in finding a collision partner. For the simple fcc and bcc metals, for example, the usual lists include both first and second neighbors, that is, 18 and 14 atoms, respectively. Lists containing only first neighbors are quicker to search, but must be searched more often because of the probability of finding no suitable collision partner. On the other hand, the description of the crystal K_2ReCl_6 required listing 124 atoms of 9 different types.

The procedure for searching the crystal is illustrated in Fig. 4(a). The projectile P, near which is the associated lattice site R, moves in the direction $\vec{\lambda}_0$. Using the list of atoms neighboring R, the position of the site T is generated and the following quantities are evaluated:

$$\zeta = \vec{\lambda}_0 \cdot \Delta\vec{x}, \tag{20}$$

$$s^2 = \zeta^2 - |\Delta\vec{x}|^2. \tag{21}$$

If $\zeta > \zeta_{min} \geq 0$, the site T is in the correct direction to be the partner of P in a collision. The previous collision of P provided the value of ζ_{min} so that multiple collisions at the same site are avoided. If the impact parameter $s > s_{max}$, then T is regarded as too far from the path of P to produce a significant deflection. The value of s_{max} is chosen large enough so that in no part of the crystal will a projectile be free of the influence of surrounding atoms, but small enough to avoid too many collisions involving very small energy transfers. After a collision has been completed, following the procedures of Sec. II, the new direction of motion of P is
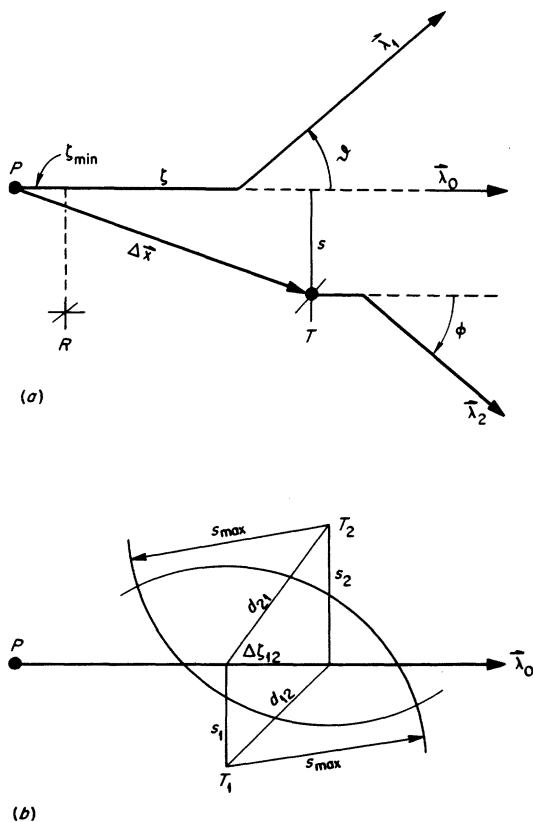

(a)

(b)

FIG. 4. (a) Basis of the crystal searching procedure. (b) The criteria for simultaneous collisions.
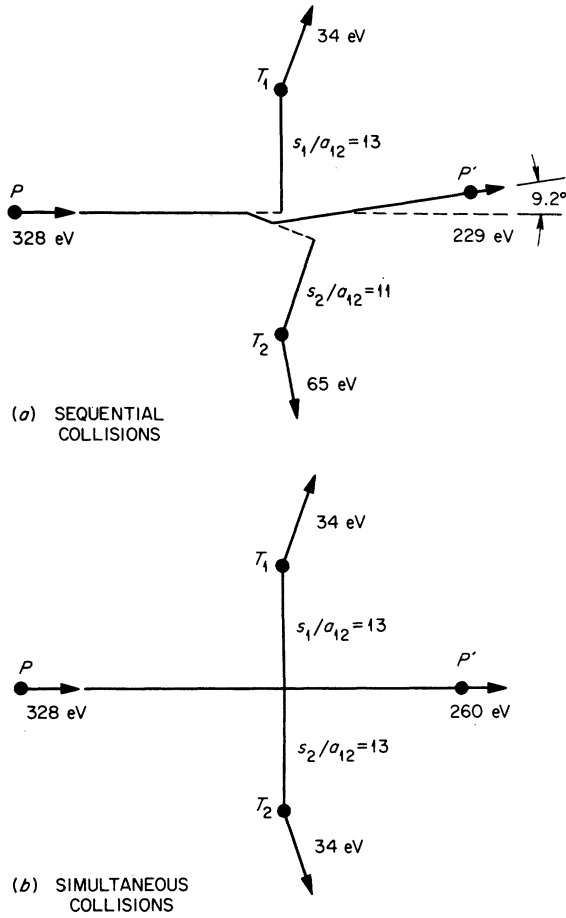
FIG. 5. Comparison of the sequential and the simultaneous treatments of a three-particle encounter. The scatterings are based on the Molière potential (Ref. 29). The example corresponds roughly to the motion of a Cu atom along a Cu $\langle 100 \rangle$ channel axis.

$$\vec{\lambda}_1 = [\cos\vartheta + (\zeta/s)\sin\vartheta]\vec{\lambda}_0 - [(1/s)\sin\vartheta]\Delta\vec{x} \, . \quad (22)$$

If the target is displaced, its direction of motion is

$$\vec{\lambda}_2 = [\cos\phi - (\zeta/s)\sin\phi]\vec{\lambda}_0 + [(1/s)\sin\phi]\Delta\vec{x} \, . \quad (23)$$

The projectile and target are moved to their new positions and the search procedure is repeated. The lattice site T will now replace R as the center for generating the crystal.

It is characteristic of recoil trajectories in crystals that they often pass near the centers of arrays of two or more symmetrically disposed target atoms. Occurences of this kind are especially important in connection with channeling and replacement sequences. The interaction of recoils with symmetric rings of atoms has been studied by Weijsenfeld[39] and by Anderson and Sigmund.[40] Unfortunately, their treatments are not valid when the encounter is asymmetrical. The procedure for sensing such events is illustrated in Fig. 4(b). When more than one potential target atom meets the cri-

teria described above, the first of these along the path of the projectile is selected, say T_1 in the figure. Then, for each of the other potential targets, the program evaluates

$$\Delta\zeta_{1i} = \zeta_i - \zeta_1,$$

$$d_{1i}^2 = s_1^2 + (\Delta\zeta_{1i})^2, \quad d_{i1}^2 = s_i^2 + (\Delta\zeta_{1i})^2.$$

If $\Delta\zeta_{1i} < \zeta_m$, $d_{1i} < s_{max}$, and $d_{i1} < s_{max}$, the second collision is regarded as simultaneous with the first. Each of the set of simultaneous collisions is carried out as if it were occurring alone. The several deflections of the projectile are then added vectorially. This procedure is compared with sequential treatment of the collisions for a simple example in Fig. 5. The sequential procedure will actually introduce an instability into the motion of a well-channeled particle, as well as increasing its energy loss rate. The simultaneous collision procedure used here avoids the instability, but underestimates the energy loss, since the free recoil of the projectile, assumed in treating the single collisions, cannot in fact occur. The occurrence of simultaneous collisions in the program can be controlled by adjusting the values of ζ_m and s_{max}. Because of the way in which simultaneous collisions are treated, it can happen that the energy of a projectile after a collision is calculated as negative. When this occurs, all quasielastic energy transfers and inelastic energy losses are scaled proportionately so that the projectile energy just vanishes. The procedure outlined for nearly simultaneous collisions has given unrealistic results in rare instances. These events have been detected only at low energies and are examples of failure of the binary collision approximation. No completely satisfactory strategy for dealing with this problem has been devised. Beeler's program[12] dealt with all collision sets in a strictly sequential manner.

A simple model of thermal vibrations is included in the program as an option. Since the vibrations are executed very slowly compared to the time of a single collision, it is sufficient to regard them as producing randomly displaced but static lattice atoms. The displacement parallel to each of the three Cartesian axes is distributed according to a Gaussian. The mean square displacement is based on the Debye model,[41] the only parameters required being the temperature and a value of Θ_D for each type of lattice site. For speed, the Gaussian deviates are generated by a table-look-up procedure. Note that no correlations occur between neighboring atomic displacements. The inclusion of thermal vibrations complicates the search procedure, especially when the amplitudes are large, by making it more difficult to avoid multiple collisions at a single site. These problems are minimized by using a value of ζ based on the lattice-site position,

instead of the thermally displaced atom position, for the search procedure alone. For all other applications, the actual atom position defines the value of ζ. In our preliminary calculations,[3] this modified procedure was not used and led to some erroneous conclusions about temperature effects on cascade production. It may be noted here that Beeler's program[12] did not include thermal vibrations.

The target crystal is allowed to have two parallel surfaces of any desired orientation, a specified distance apart. One surface, which may be irradiated by a beam of ions, is defined by the direction of its normal and of one lattice point contained in it. The location of any particle with respect to either surface is easily found by vector operations similar to Eq. (20). This feature of the program is not needed in the present calculations, but has been used in related work.[4]

The search for potential target atoms includes a check of the possibility that a site has already been vacated. This can be a vacancy introduced into the crystal before the displacement of the primary recoil or it can be a vacancy produced by a displacement event. Interstitial atoms may also be introduced into the crystal at the beginning of the calculation and, if present, are included in the search procedure. Cascade atoms may also be included in the list of potential target atoms, after they have come to rest. However, events in which such atoms are redisplaced occur only at very low energies and have not been allowed in most of the work reported here. In Beeler's calculation,[12] stopped cascade atoms were always immediately available as target atoms.

The development of the cascade in time was simulated by always computing the next collision of the fastest particle currently in the cascade. This procedure was altered only when a sequence of replacement collisions was detected. Here, since the target receives nearly all of the projectile energy, it is followed immediately. Our procedure differs from that used by Beeler. In his program,[12] every atom currently in the cascade was followed through one collision before any atom made another collision. The faster of two particles coming from a particular collision was followed first. This procedure probably does not represent the temporal development of the cascade very well and may be partly responsible for differences between his results and ours.

Provision is made for the truncation of certain events strongly influenced by lattice correlations. Recoils that make a large number of successive small angle scatterings are assumed to be channeled and their trajectories are abbreviated. In the present calculations, channeling plays a comparatively minor role and no trajectories required truncation. It is much more significant in calculations simulating ion bombardment of monocrystal surfaces.[4] Long sequences of replacement collisions are also detected and abbreviated. In contrast to channeling, these sequences occur at low energies, with a probability which is a strong function of the displacement threshold value chosen. The trajectories of particles are also terminated when they escape from either surface of the crystal.

The primary recoil atoms which generate a displacement cascade may have initial properties which are definitely assigned or they may be selected by stochastic techniques. In the latter case, the primaries may be started at a particular site with their initial velocities chosen from an isotropic distribution. Alternatively, if an ion beam is to be simulated, the primaries may have a specified initial direction, but make impacts at random on the target surface. The former choice was made in all of the present calculations.

V. DISPLACEMENT MODEL

Since the binary collision procedure used in MARLOWE cannot deal directly with questions of defect stability and interactions, it is necessary to include a model describing the conditions under which atoms may become permanently displaced from lattice sites. The program allows considerable flexibility in defining this model, with a view to studying its influence on the results of the calculations. Consider a collision from which the original projectile emerges with kinetic energy E_1, after transferring kinetic energy T to the target atom [cf. Eqs. (8) and (10)]. The target is displaced if its energy exceeds a sharp threshold energy E_d.[42] It may be required at the same time to overcome a binding energy $E_b \le E_d$. Thus, if $T > E_d$, the target is added to the cascade with kinetic energy

$$E_2 = T - E_b. \tag{24}$$

The atoms in the cascade are followed as long as their energies exceed a preassigned value E_c. No limitation is placed on the relation between E_c and E_d. The projectile is deemed to replace the target on its lattice site when $T > E_d$ and E_1 is less than the lesser of E_c and E_d. This definition is a slight modification of that of Kinchin and Pease.[43] If the arriving projectile is of the correct chemical type to occupy the vacated lattice site, the replacement is termed *proper*; otherwise, it is *improper*. No attempt is made to force stopped projectiles to occupy particular locations. Both interstitials and replacing atoms are left at the turning points of the collisions in which their energies pass below E_c. This procedure is argued from the fact that these abandoned particles still have kinetic energy which they must dissipate before they adopt well-defined positions. The time required for this energy dissipation exceeds the time needed to generate the cascade. A corollary of this argument is that interactions between cascade particles should be omitted. Beeler's procedure[12-16] again differed

from ours. His stopped cascade atoms were placed on a vacant lattice if one was available (see below) or else in a specified interstitial location. For the latter, the octahedral site was chosen in the simple fcc and bcc metals.

After all cascade atoms have come to rest, that is, when no particle remains with energy greater than E_c, a distribution function is constructed of the separations between the cascade atoms and the vacancies. Each vacancy is paired uniquely with a displaced atom in such a manner that the smallest separation is found first, then the next smallest, and so on, until the list of defects is exhausted. This pairing may be restricted to vacancies and to cascade atoms which have come to rest interstitially. Alternatively, the sites and atoms involved in replacement collisions may also be used in pairing. The resulting distribution function $N(r_v)$ gives the number of pairs of separation exceeding r_v. Identifying r_v with the capture radius of a vacancy,[44] $N(r_v)$ may be used to discuss the recombination of point defects on the principle that the pairs of smallest separation recombine first.

The displacement model corresponds to the familiar one of Kinchin and Pease[43] if $r_v = E_b = 0$, $E_c = E_d$, and E_d is chosen to represent the threshold energy for producing *permanent* displacements, traditionally about 25 eV.[42] If $r_v = 0$ and $E_b = E_c = E_d$, the model corresponds to that of Snyder and Neufeld.[45] Beeler[16] has pointed out that these models assume that the defects produced are isolated from each other. When this is not so, a simple displacement energy threshold is probably not appropriate. Beeler chose $E_b = E_c = E_d$, with E_d twice the heat of sublimation of the metal (7 eV for Cu), combined with a recombination region based on the machine calculations of Vineyard et al.[6,7] Although this region was nonspherical, it corresponded approximately to $r_v = 1.36a_0$ in Cu and $1.53a_0$ in Fe, where a_0 is the cubic cell edge. In the calculations presented here, $E_b = 0$ always. Comparisons will be made between calculations in which there is no recombination and $E_d \sim 25$ eV and calculations in which $E_d \sim 5$ eV and close defect pairs are recombined after generating the cascade. In the latter case, E_d no longer represents a threshold for permanent displacements, but is primarily a convenience in computing, to avoid consuming large amounts of time and storage in dealing with inconsequential low-energy recoils.

VI. LIMITATIONS OF THE BINARY-COLLISION APPROXIMATION

Before turning to a discussion of some results of calculations using MARLOWE, it is appropriate to make a few remarks about limitations of the binary collision approximation on which the model is based. One question is the effect of replacing the real par-

ticle trajectory by its asymptotes in the L system. According to Eqs. (11) and (12) and Fig. 1, the minimum distance between the L asymptotes is $s \sec\frac{1}{2}\theta$. Thus, a measure of the deviation between the exact and the asymptotic trajectories is the ratio of this quantity to the actual apsis: a substantial deviation from unity indicates failure of the model approximation. This ratio is plotted in Fig. 6 for the Molière potential and for three potentials that can be treated analytically. The curves show the gradual transition of the Molière scattering from hard-core-like at low energies to Coulomb-like at high energies. The apsidal ratio differs from unity most seriously in head-on collisions and at high energies, but then the apsides themselves are small so that the particles reach their asymptotic trajectories again before encountering their next collision partners.

The successive binary collisions can be regarded as isolated as long as x_1 and x_2 (compare Fig. 1) are small compared to typical lattice distances. When this is no longer so, part of each encounter is strongly influenced by additional atoms in the crystal. Restricting the discussion to elastic collisions between particles of equal mass, the condition is that τ and $(s \tan\frac{1}{2}\theta - \tau)$ each be small compared to lattice distances. The time integral is tabulated.[28] For central collisions, the matching potential method of Leibfried and Oen[46] may be used to show that

$$\lim_{s \to 0} s \tan\tfrac{1}{2}\theta \approx R\left(\frac{1+\Phi(R)}{\Phi(R)-R\Phi'(R)}\right)^{-1}. \qquad (25)$$

When the energy is sufficiently low, the factor in parentheses approaches unity, in which limit Eq. (25) agrees with the corresponding result for the hard core approximation. Figure 7 displays the dependence of x_1 and x_2 on the collision energy for head-on collisions. The binary collisions can be fairly well isolated as long as x_1 is less than, say, half the nearest-neighbor distance in the crystal. As
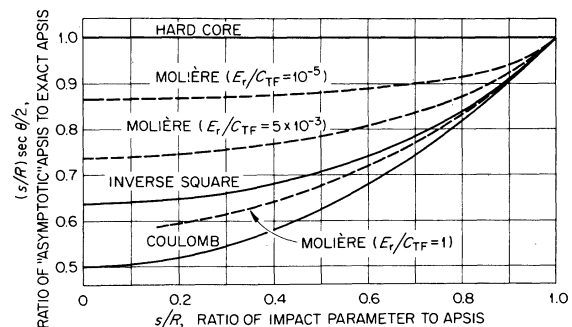

FIG. 6. Comparison of the asymptotic L trajectory with the exact trajectory for several interatomic potentials. $C_{TF} = Z_1 Z_2 e^2 / a_{12}$. The three energies correspond roughly to 3.3 eV, 1.6 keV, and 328 keV for Cu–Cu collisions.

the figure shows, this limit is encountered at about 9 eV for Cu collisions and about 33 eV for Au collisions. Below these energies isolation of the collisions becomes much less satisfactory. Note that no limitation is encountered with respect to x_2. The situation is reminiscent of that which occurs in a system of hard spheres when their diameters become comparable to the distances between their centers. In the present model, occasional events are encountered in which x_1 is larger than the original separation between the collision partners. If no alteration were made in the program, the projectile would actually back up to the deflection point. This reverse motion is (optionally) prevented in the program. The result is that low energy projectiles tend to stop rather suddenly in a manner that is perhaps not too unreasonable.

It should be clear from Fig. 7 and from Table I as well that the binary collision approximation fails in a serious manner at low recoil energies. In spite of certain *ad hoc* features of the present model designed to cope with this failure, results of the calculations which depend sensitively on the motions of low energy particles are probably only of qualitative significance. Features of this kind must in future be investigated with programs of the molecular dynamics type[6-10] to determine the importance of cooperative effects. On the other hand, the present program is capable of outlining those low-energy motion problems which are likely to be significant experimentally, as long as the necessary caution is exercised in interpreting their quantitative aspects.

VII. CALCULATIONS WITH A THRESHOLD ENERGY

The calculations presented first were intended to study the effects of altering some of the parameters of the computer model, to compare the results with
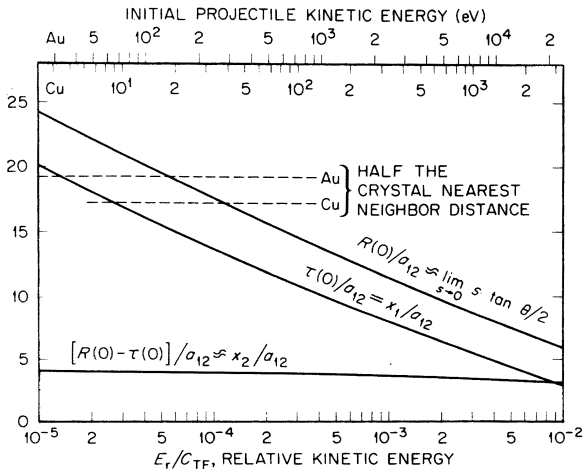

FIG. 7. Dependence of x_1 and x_2 on the collision energy, for head-on collisions using the Molière potential.

TABLE III. Model parameters used in calculations with an energy threshold.

	Cu	Au	Fe
Lattice constant, a_0, Å	3.615	4.079	2.866
Maximum impact parameter, s_{max}/a_0	0.51	0.51	0.71
Simultaneous collision control, ζ_m/a_0	0.25	0.25	0.25
Displacement threshold, E_d, eV	25	35	25
Debye temperature, Θ_D, K	315		

the analytical theories, and to compare the present calculations with those of Beeler.[12-16] All of the calculations presented in this section used a displacement threshold energy of the Seitz[42] type to define permanent displacement of the lattice atoms. The screening lengths in the potential were those of the second column in Table II. Except as noted below, the other model parameters were those listed in Table III. In each case, the primary recoil directions were distributed uniformly over $\frac{1}{48}$ of the unit sphere.

Figure 8 shows distribution functions of the number of Frenkel pairs produced in Cu for three different primary recoil energies. At the two higher energies a pronounced tail is seen on the low-defect-number side of the histograms. In most of these events, the primary recoil was channeled; more rarely, another cascade particle was channeled. The channeled atoms are associated with a reduced number of displacements, an increased particle range, and a large loss of energy by inelastic processes. The channeling probability is about 1% at each energy, a result comparable to that obtained in range calculations using other potentials.[18] Ignoring these tails, the distributions are closely Gaussian, as shown by analysis of their third and fourth moments. The dispersion shown in Fig. 8 has two distinct sources. First, different cascades experience different amounts of inelastic energy loss; that is, there is straggling of the damage energy[2]

$$\hat{E} = E_0 - \hat{Q}, \tag{26}$$

where $\hat{Q}$ is the total energy lost from a cascade by inelastic processes. Second, there are fluctuations in the number of defects produced for a particular value of $\hat{E}$. Leibfried[47] has discussed this problem using hard core scattering and the Kinchin-Pease sharp displacement threshold model. He finds the scaled variance

$$(\langle \nu^2 \rangle - \langle \nu \rangle^2)/\langle \nu \rangle = 4\ln\frac{4}{3} - 1 = 0.15073 \tag{27}$$

for $E_0 > 4E_d$. Here $\langle \nu \rangle$ and $\langle \nu^2 \rangle$ are, respectively, the mean and mean-square numbers of Frenkel pairs produced. The scaled variance is shown in Fig. 9 for the calculations of Fig. 8 and similar ones at higher energy. Assuming that the two contributions to the straggling of ν are independent,
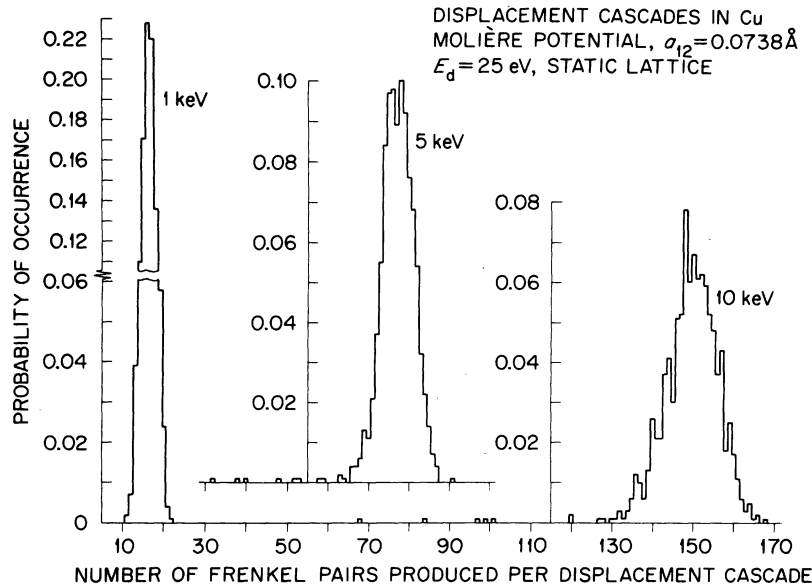
FIG. 8. Distribution functions of the numbers of Frenkel pairs produced in displacement cascades in Cu. Each histogram includes 1000 cascades.

the scaled variance can be corrected for the effect of inelastic losses. As Fig. 9 shows, the corrected values are only slightly higher than Leibfried's hard-core calculation. Lehmann[48] has shown by an example that increasing the relative importance of forward scattering over that in the hard-core approximation leads to an increase in the scaled variance, Eq. (27). This makes it clear that the use of realistic scattering from the Molière potential is responsible for the calculated result. That the result is no larger and changes no more than it does with primary recoil energy reflects the overriding importance of the low-energy scattering law in problems of this type.[1,2,49]

Since the machine computation is fairly time consuming (for example, the 50-keV results in Fig. 9 required about 23 sec per cascade on an IBM System/360, Model 91 machine), a thorough exploration of the effects of the various model param-

eters must be limited to small samples. It is clear from the distributions in Fig. 8 that such small samples can give reliable estimates of some quantities. Thus, at 10 keV, a sample of 20 cascades should yield only about a 1% uncertainty in the value of $\langle \nu \rangle$. Care must be exercised in using small samples in some applications, however. Calculations of sputtering yields,[4] for example, require quite large samples to achieve good precision, counting statistics being roughly applicable.

The mean total inelastic energy loss $\langle \hat{Q} \rangle$, as calculated for cascades in Cu at various energies, is shown in Fig. 10. The machine calculations are compared with the energy-partition theory of Lindhard et al.[50] The predictions of this theory are shown using Lindhard's original estimate (cf. Ref. 2) of his parameter
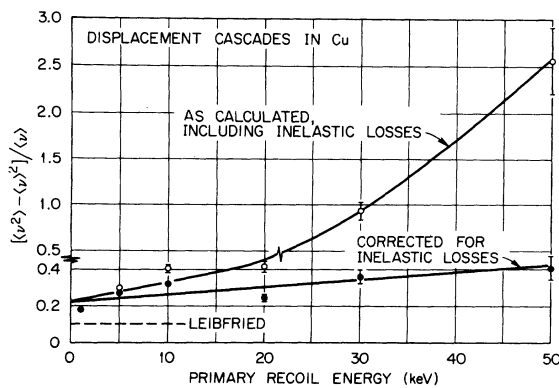
$$k = 0.876\ Z_1^{1/6}$$

FIG. 9. Scaled variance for Frenkel pair production in Cu. The error bars reflect the reduced sample sizes for $E_0 > 20$ keV.
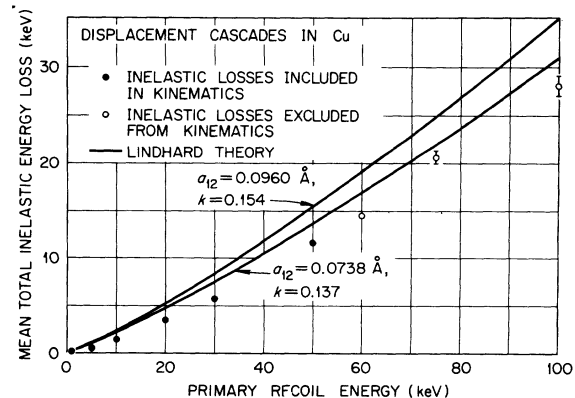

FIG. 10. Inelastic energy losses calculated for cascades in Cu, compared with the theory of Linhard et al. (Ref. 50).

and the Firsov screening length. It is also shown using the value of a_{12} employed in the machine calculation and the estimate[2] $k = 0.137$, corresponding to the Firsov inelastic-loss theory.[36] The discrepancy between the latter and the MARLOWE results is accounted for by the differences in the treatment of inelastic losses at low energies. As indicated in Fig. 3, the low-energy inelastic losses in the machine calculation are much smaller than those in the Lindhard theory. In the latter, a Cu atom recoiling at the displacement threshold ($E_d = 25$ eV) will lose ~2 eV in electron excitation. This small amount, summed over the large number of particles in a high-energy cascade which are eventually set into motion, accounts for the difference in Fig. 10 between the Lindhard theory and MARLOWE. Even though the inelastic losses in the machine program at low energies are small, they are not negligible. Thus, $\langle \hat{Q} \rangle$ depends not only on the primary recoil energy E_0, but also on the projectile cutoff energy E_c. This dependence is fairly weak, but must be borne in mind. The value of $\langle \hat{Q} \rangle$ is scarcely affected by whether or not the individual contributions are included in the collision kinematics. As an example, at 10 keV, $\langle \hat{Q} \rangle$ was 1429 ± 8 eV in the former case and 1407 ± 7 eV in the latter. There was greater straggling of $\hat{Q}$ when the inelastic losses were included in the kinematics.

It is convenient to discuss the production of Frenkel pairs in a cascade in terms of the displacement efficiency κ, defined by

$$\langle \nu \rangle = \kappa \langle \hat{E} \rangle / 2E_d . \qquad (28)$$

The dependence of κ on the primary recoil energy, the target temperature, and several parameters of the computational model has been investigated for several different targets. The results are summarized in Figs. 11 and 12. The former shows the effects of changing the values of E_d and E_c. When E_c is lowered from $2E_d$ to E_d, there is no change the number of defects produced, but the damage energy decreases because of the slightly increased inelastic losses. This produces a small increase in κ. As E_d is decreased, a small decrease in κ occurs. This appears to reflect the increasing importance of replacement collision sequences, and hence of subthreshold energy transfers, at low projectile energies. Further work is in progress to study this point in more detail. Figure 12 displays the primary-recoil-energy dependence of κ for several materials and for alterations of several model parameters. The calculations for Cu show the effects of changing E_c, of the method of treating inelastic losses, and of target temperature. The calculations for Fe show the effects of omitting inelastic losses altogether, of omitting "simultaneous" collisions, and of ignoring the time integral. It is clear from the figure that none of these alterations

is of any significance and that a constant value, κ ~0.86, represents all of these calculations rather well. This conclusion is in agreement with the predictions of analytical cascade production theories.[1,2] Figure 12 also shows values of κ calculated for Au, for cascades produced by Cl recoils in K_2ReCl_6 (cf. Ref. 5), and for cascades produced by an Ar atom incident on the (100) surface of a thin Cu crystal.[4] The decrease of κ with increasing Ar energy in the latter case stems from an increase in the energy carried out of the target by sputtered atoms. Our earlier claim[3] that the inclusion of thermal vibrations leads to a decrease in the displacement efficiency is not supported by the present calculations. The effect was a consequence of occasional instances of multiple collisions at a single site, improperly included when a previous target vibrated forward along the trajectory of a projectile and was hit again. Such events were eliminated by using the lattice site in the search procedure (cf. Sec. IV).

Whereas the present calculations always show κ < 1 in agreement with analytical theories,[1,2] Beeler's calculation[16] shows $\kappa > 1$; that is, he obtained more displacements than the analytical models predict. If κ is defined in terms of the Kinchin-Pease[43] model as in Eq. (28), his results correspond to $\kappa = 1.04$ in Cu and 1.06 in Fe (cf. Table VI of Ref. 16). Even higher values would be deduced for a Snyder-Neufeld[45] model. Of the several differences between our program and Beeler's, only the different sequencing of collisions and the possibility of cascade atoms being redisplaced after coming to rest can be responsible for the differing results. In particular, in Beeler's program, stopped interstitial atoms can be produced from the beginning of cascade development. This can lead to debris produced by slow recoils interfering with the progress of fast ones. In our program, on the other hand, stopped interstitial cascade atoms can appear only near the end of cascade development. The fast particles tend to run away from the slow
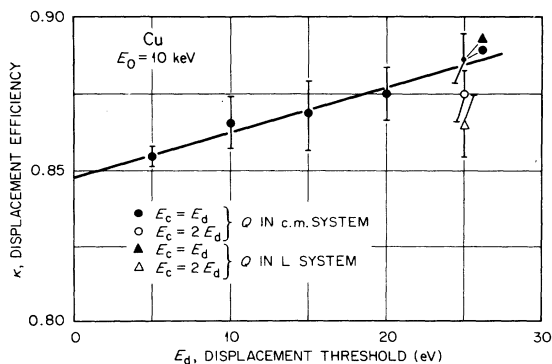

FIG. 11. Effects of E_c and E_d on displacement efficiencies calculated for 10-keV cascades in Cu.
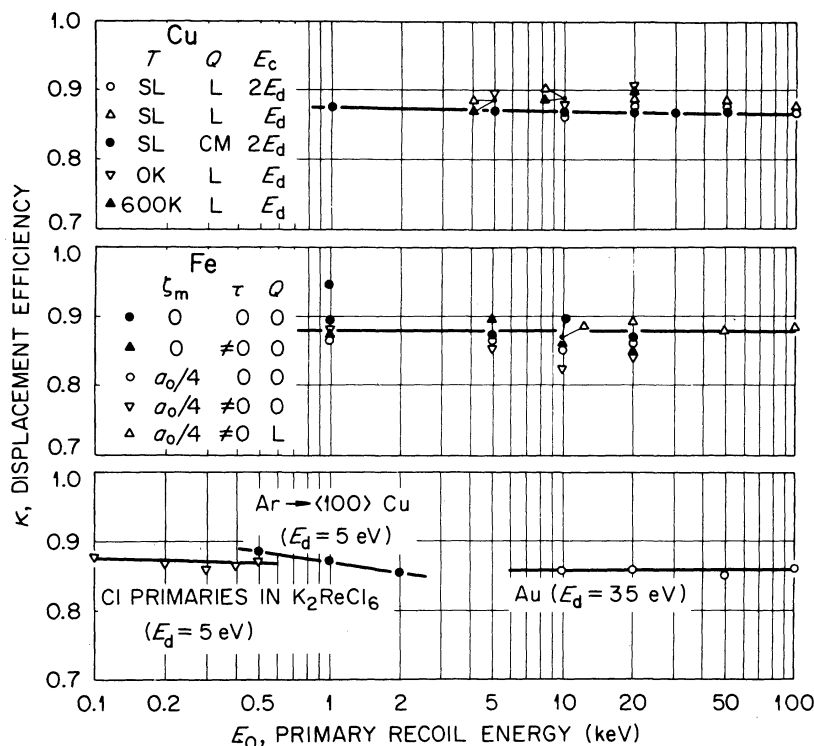
FIG. 12. Displacement efficiencies calculated for cascades in several materials, showing the effects of altering various model parameters.

ones into undamaged crystal. Thus, Beeler's cascades might be rather more dense than ours, other things being equal, and show considerably more in the way of interference effects. The greater density of Beeler's cascades has been noted by Doran.[51]

VIII. CALCULATIONS INCLUDING RECOMBINATION EFFECTS

The calculations presented in Sec. VII were based on a threshold energy criterion for permanent displacement of lattice atoms. These results must now be contrasted with calculations based on a distance criterion for permanent displacement. Figure 13 shows the mean number of Frenkel pairs produced in low-energy cascades according to each of three different models for Cu. The first of these is the threshold model described in Sec. VII. The parameters of the other two models have been adjusted to produce approximately the same number of stable defects as model 1 near 50-eV primary recoil energy. In model 2, the same threshold energy controls the addition of new particles to the cascade as in model 1, but the projectiles are allowed to slow down to a much lower energy before being regarded as stopped. This change brings the interstitials to more realistic distances from the vacancies, but also decreases the number of replacement collisions. A small vacancy-capture radius is used to compensate for this reduction. In model 3, a low value of E_d is used, greatly increasing the number of nascent defects, but this

is offset by a suitable choice of r_v. The closely similar dependence of $\langle \nu \rangle$ on E_0 in the three models will be evident. It is clear that for low energy recoils, the three models are equivalent.

The behavior of the three models is shown at higher energies in Fig. 14. Here the mean damage energy per Frenkel pair, that is $\langle \hat{E}/\nu \rangle$, is plotted as a function of $\langle \hat{E} \rangle$. The straight lines were fit to the calculated points by the method of least squares, using the points shown for models 2 and 3, and points extending to 50 keV for model 1. The linearity of the plots is made plausible by a simple analogical argument based on defect annihilation kinetics. Since there are equal numbers of nascent vacancies and interstitials, the differential equa-
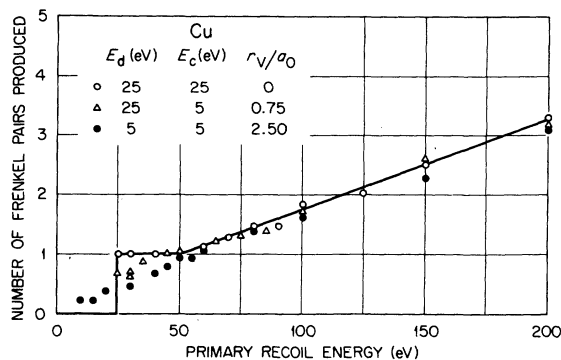

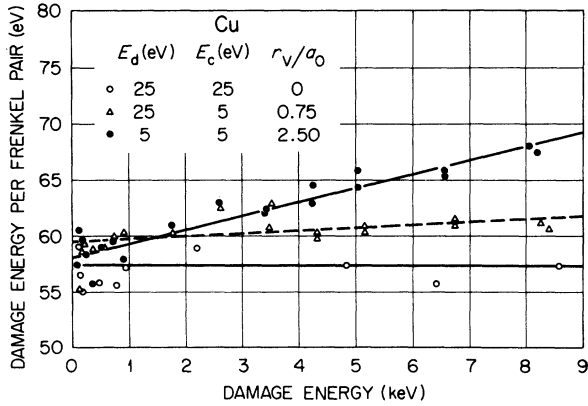FIG. 13. Comparison of low-energy cascades in Cu for three different displacement models.

FIG. 14. Comparison of high-energy cascades in Cu for three different displacement models.

tion describing their annihilation is $\dot{c} = -kc^2$, with $c(t=0) = c_0$, where c is the concentration of point defects of either kind. The integral of this equation is

$$c(t) = c_0/(1 + kc_0 t).$$

Extending this equation by analogy to the total number of point defects and noting that the number of nascent defects is proportional to the damage energy, we may write

$$\langle \hat{E}/\nu \rangle = \alpha + \beta \langle \hat{E} \rangle . \qquad (29)$$

Comparison of Eqs. (28) and (29) shows that

$$\alpha = 2E_d^*/\kappa, \qquad (30)$$

where E_d^* is the traditional displacement threshold energy. Equation (29) represents our calculations very well, the mean deviation of the points from the lines being about $\pm 1.6\%$ for model 2 and $\pm 1.9\%$ for model 3. Since model 3 is very similar to Beeler's model, our results can be compared with his by fitting ours to the same logarithmic function which he used[16]:

$$\langle \nu/\hat{E} \rangle = \gamma_0[1 - \gamma_1 \ln\langle \hat{E}_{keV} \rangle] . \qquad (31)$$

As Table IV shows, the values of the slope parameter γ_1 from the two calculations are in good agreement, the 16% difference being ascribable to the differences in threshold and recombination region. On the other hand, the large difference in the intercept parameter γ_0 may be explained by the different choices of the binding energy E_b. Beeler's model is of the Snyder-Neufeld type,[45] where the number of defects is expected to be roughly inversely proportional to $3E_d$, while ours is of the Kinchin-Pease type,[43] where the expected proportionality constant is about $2E_d$. Taking into account the different values of E_d, the expected ratio between the two calculations is about 2.1, in fair agreement with the ratio 1.7 from Table IV. The agreement would be

TABLE IV. Comparison of the present calculations for Cu with those of Beeler (Ref. 16).

	Present work	Beeler
Binding energy E_b, eV	0	7
Displacement threshold, E_d, eV	5	7
Vacancy capture radius, r_v/a_0	2.5	~1.36[a]
Intercept, γ_0, keV^{-1}	16.55 ± 0.11	9.65
Slope, γ_1	0.0401 ± 0.0049	0.0315

[a]Recombination region was nonspherical.

improved if the comparison were made at a lower energy than 1 keV.

In Fig. 15, the effects of varying the vacancy capture radius are shown. The nascent cascades are the same ones used in model 3 above. The linear dependence of $\langle \hat{E}/\nu \rangle$ on $\langle \hat{E} \rangle$ is shown for all values of r_v. However, as Fig. 16 shows, the slope of the line saturates for large capture radii. No evidence of saturation appears in calculations related to model 2. The principal difference between cascades with $E_d = 25$ eV and those with $E_d = 5$ eV is the greater density of displaced atoms along the tracks of the high-speed recoils in the latter case. This may be related to the partial nuclear stopping cross section
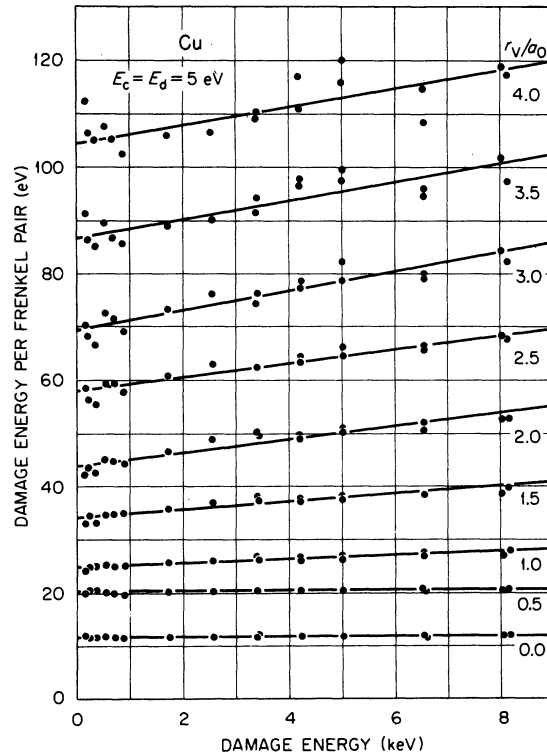

FIG. 15. Effect of the vacancy capture radius on the damage energy per Frenkel pair in Cu.
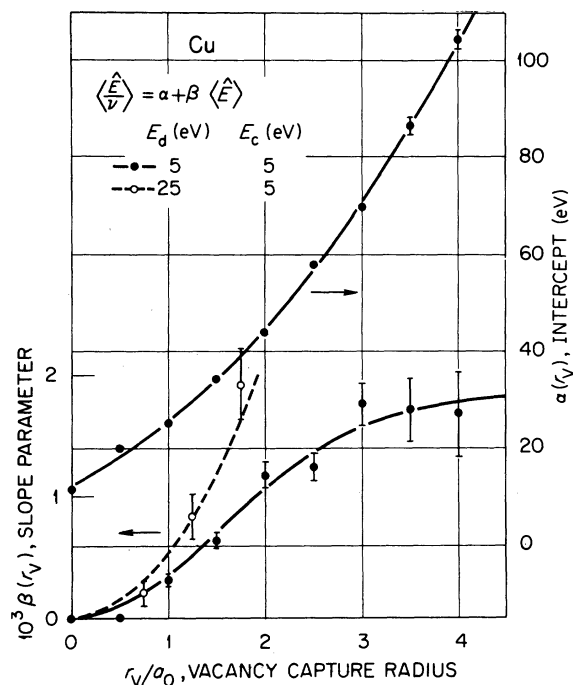
FIG. 16. Parameters of the relation between $\langle \hat{E}/\nu \rangle$ and $\langle \hat{E} \rangle$ for Cu.

$$S_n(E, E_d) = 2\pi \int_0^{S_d} s\, T(s, E)\, ds, \qquad (32)$$

where $T(s_d, E) = E_d$. As E_d is lowered, a great increase occurs in the density of low energy recoils along a track and it is the interference among these recoils which produces the recombination effect. Saturation of the effect comes about when r_v is

large enough that the instability region around a vacancy contains more than one interstitial.

It must be admitted that the justification of Eq. (29) is not especially compelling, so that it cannot be said with certainty to be more appropriate than Eq. (31). They differ quite sharply in their predictions for very high-energy cascades, however. For example, for 100-keV Cu recoils, Fig. 10 gives $\langle \hat{E} \rangle = 72$ keV. Using Eq. (29) and the model-3 parameters of Fig. 14, the predicted number of Frenkel pairs is about 490; using Eq. (31) and the parameters of Table IV, the predicted number is about 990. The superiority of the one function or the other could be determined by calculations for high-energy recoils and low values of E_d and E_c, but these would be very costly in machine time and memory requirements with the present program. On the other hand, the whole question of the appropriateness of the calculations presented in this section must be considered. Since the recombination effects reported are connected with the behavior of low-energy recoils, the limited validity of the binary-collision approximation must be remembered. It would be very helpful to have molecular dynamics calculations available in which short sections of high-speed recoil track were simulated, so that the foundations of the present calculation could be more firmly based.

IX. DISCUSSION

A long-standing problem in radiation damage is the serious divergence between experimental and theoretical estimates of the number of Frenkel pairs produced in pure metals by irradiation, especially with fast neutrons and other energetic

TABLE V. Comparison of experimental and theoretical resistivity changes induced in Cu at 4.2 K.[a]

	Electrons (1.4 MeV)	Neutrons Thermal	Fission	Deuterons (9 MeV)
(A) Ionization threshold and displacement threshold ($E_d = 22$ eV) (Ref. 52)				
Mean primary energy	45 eV	388 eV	64 keV	270 eV
Mean damage energy	45 eV	388 eV	27.4 keV	270 eV
$\Delta\rho_{calc}/\Delta\rho_{obs}$	1.2	2.0	4.3	3.6
(B) Lindhard ionization losses and displacement threshold ($E_d = 22$ eV)				
Mean primary energy	45 eV	374 eV	$\cdots$	
Mean damage energy	45 eV	314 eV	22.9 keV	
$\Delta\rho_{calc}/\Delta\rho_{obs}$	1.2	1.6	3.6	

(C) Lindhard ionization losses and unstable Frenkel pair collapse [energies as in (B)]

r_v/a_0	$\Delta\rho_{calc}/\Delta\rho_{obs}$	$\Delta\rho_{calc}/\Delta\rho_{obs}$	$\Delta\rho_{calc}/\Delta\rho_{obs}$	
2.0	1.2	1.6	2.3	$\dfrac{\Delta\rho_{calc}}{\Delta\rho_{obs}}$
2.5	0.9	1.2	1.8	
3.0	0.7	1.0	1.5	

[a]Frenkel pair resistivity $\rho_F = 2.0$ $\mu\Omega$ cm/at.%.

heavy particles. The calculations presented in the previous section provide a possible solution to the difficulty. Holmes[52] has compared the electrical resistivity changes induced in Cu at 4.2 K by various irradiations with the theoretical values based on a Kinchin-Pease sharp displacement threshold. The fast-neutron result was corrected for electronic energy losses by assuming all recoil energy above about 63 keV to be lost in this way.[2,42,43,52] Holmes's comparison is shown in the first part of Table V. In the second part of the table, the electronic loss correction is made by the Lindhard theory.[50] The mean recoil energy for the thermal-neutron case is a revised value.[53] The damage energy for the fission-neutron case uses values calculated recently for monoenergetic neutrons,[54] averaged over the ^{235}U fission spectrum.[55] The agreement between theory and experiment is somewhat improved, but not dramatically. The third part of Table V shows the result of using the recombination model of Sec. VIII, that is, Eq. (29) with the parameters of the smooth curves in Fig. 16. The approximation

$$\langle \nu \rangle = \langle \hat{E}/(\alpha + \beta \hat{E}) \rangle \approx \langle \hat{E} \rangle/(\alpha + \beta \langle \hat{E} \rangle) \tag{33}$$

has been used, where the averaging is over the distribution of $\hat{E}$. This approximation causes an overestimate of $\langle \nu \rangle$, especially for the fission neutron case. In spite of this, the recombination model shows a striking improvement over the energy threshold model. Further improvement might be achieved by avoiding the approximation (33) as well as by altering various parameters of our calculational model, for instance, the potential parameters. The time would also seem to be ripe for a careful critical examination of the experimental data, with the objective of extending comparisons like those in Table V to other materials on as reliable a base as possible.

ACKNOWLEDGMENTS

---

*Research sponsored in part by the U.S. Atomic Energy Commission under contract with Union Carbide Corp.

†Present address: Energy Division, Organization for Economic Cooperation and Development, 2, rue André-Pascal, Paris 16e, France.

[1]P. Sigmund, Revue Roum. Phys. 17, 823 (1972).

[2]M. T. Robinson, in Radiation Induced Voids in Metals, edited by J. W. Corbett and L. C. Ianniello, U.S. Atomic Energy Commission, CONF-710601 (U.S. GPO, Washington, D.C., 1972), p. 397.

[3](a) I. M. Torrens and M. T. Robinson, in Ref. 2, p. 739; (b) and in Interatomic Potentials and Simulation of Lattice Defects, edited by P. C. Gehlen, J. R. Beeler, Jr., and R. I. Jaffee (Plenum, New York, 1972), p. 423.

[4]M. T. Robinson and I. M. Torrens, International Conference on Ion-Surface Interaction, Garching bei München, Germany, September, 1972 (unpublished).

[5]M. T. Robinson, K. Rössler, and I. M. Torrens, J. Chem. Phys. 60, 680 (1974).

[6]J. B. Gibson, A. N. Goland, M. Milgram, and G. H. Vineyard, Phys. Rev. 120, 1229 (1960).

[7]C. Erginsoy, G. H. Vineyard, and A. Englert, Phys. Rev. 133, A595 (1964).

[8]C. Erginsoy, G. H. Vineyard, and A. Shimizu, Phys. Rev. 139, A118 (1965).

[9]I. M. Torrens and L. T. Chadderton, Phys. Rev. 159, 671 (1967).

[10]A. Scholz and C. Lehmann, Phys. Rev. B 6, 813 (1972).

[11]D. E. Harrison, Jr., N. S. Levy, J. P. Johnson, III, and H. M. Effron, J. Appl. Phys. 39, 3742 (1968); D. E. Harrison, Jr., W. L. Moore, Jr., and H. T.

Holcombe, Radiat. Eff. 17, 167 (1973).

[12]D. G. Besco and J. R. Beeler, Jr., U.S. Atomic Energy Commission Report No. GEMP-200, February, 1963 (unpublished); ibid. GEMP-243, August, 1963 (unpublished).

[13]J. R. Beeler, Jr. and D. G. Besco, J. Appl. Phys. 34, 2873 (1963).

[14]J. R. Beeler, Jr., J. Appl. Phys. 35, 2226 (1964).

[15]J. R. Beeler, Jr., J. Appl. Phys. 37, 3000 (1966).

[16]J. R. Beeler, Jr., Phys. Rev. 150, 470 (1966).

[17]O. S. Oen, D. K. Holmes, and M. T. Robinson, J. Appl. Phys. 34, 302 (1963).

[18]M. T. Robinson and O. S. Oen, Phys. Rev. 132, 2385 (1963).

[19]O. S. Oen and M. T. Robinson, J. Appl. Phys. 35, 2515 (1964).

[20]D. V. Morgan and D. VanVliet, Can. J. Phys. 46, 503 (1968).

[21]D. V. Morgan and D. VanVliet, in Atomic Collision Phenomena in Solids, edited by D. W. Palmer, M. W. Thompson, and P. D. Townsend (North-Holland, Amsterdam, 1970), p. 476.

[22]J. H. Barrett, Phys. Rev. B 3, 1527 (1971).

[23]W. M. Gibson, Y. Hashimoto, R. J. Keddy, M. Maruyama, and G. M. Temmer, Phys. Rev. Lett. 29, 74 (1972).

[24]N. Bohr, Kgl. Danske Videnskab. Selskab, Mat. -Fys. Medd. 18, No. 8 (1948).

[25]C. Lehmann and G. Leibfried, A. Physik 172, 465 (1963).

[26]H. Goldstein, Classical Mechanics (Addison-Wesley, Cambridge, Mass., 1950), p. 58.

[27]G. Leibfried, *Bestrahlungseffekte in Festkörpern* (Teubner, Stuttgart, 1965), pp. 30–64.

[28]Z. Kopal, *Numerical Analysis* 2nd ed. (Wiley, New York, 1961), p. 367.

[29]M. T. Robinson, U.S. Atomic Energy Commission Report No. ORNL-4556, 1970 (unpublished).

[30]I. M. Torrens, *Interatomic Potentials* (Academic, New York, 1972).

[31]In Ref. 3b, especially Parts 1 and 2.

[32]G. Molière, Z. Naturforsch. A $\underline{2}$, 133 (1947).

[33]M. T. Robinson in Ref. 31, p. 281.

[34]O. B. Firsov, Zh. Eksp. Teor. Fiz. $\underline{33}$, 696 (1957) [Sov. Phys. - JETP $\underline{6}$, 534 (1958)].

[35]M. W. Thompson, Philos. Mag. $\underline{18}$, 377 (1968).

[36]O. B. Firsov, Zh. Eksp. Teor. Fiz. $\underline{36}$, 1517 (1959) [Sov. Phys. - JETP $\underline{36}$, 1076 (1959)].

[37]J. Lindhard, M. Scharff, and H. E. Schiott, Kgl. Danske Videnskab. Selskab, Mat.-Fys. Medd. $\underline{33}$, No. 14 (1963).

[38]L. C. Northcliffe and R. F. Schilling, Nucl. Data A $\underline{7}$, 233 (1970).

[39]C. H. Weijsenfeld, Philips Res. Rep. Suppl. No. 2 (1967).

[40]H. H. Andersen and P. Sigmund, Phys. Lett. $\underline{15}$, 237 (1965); Kgl. Danske Videnskab. Selskab, Mat.-Fys. Medd. $\underline{34}$, No. 15 (1966).

[41]M. Blackman, in *Handbuch der Physik*, edited by S. Flügge (Springer-Verlag, Berlin, 1955), Vol. VII, Part 1, p. 325.

[42]F. Seitz, Disc. Faraday Soc. $\underline{5}$, 271 (1949).

[43]G. H. Kinchin and R. S. Pease, Rep. Prog. Phys. $\underline{18}$, 1 (1955).

[44]H. J. Wollenberger, in *Vacancies and Interstitials in Metals*, edited by A. Seeger, D. Schumacher, W. Schilling, and J. Diehl (North-Holland, Amsterdam, 1970), p. 215.

[45]W. S. Snyder and J. Neufeld, Phys. Rev. $\underline{97}$, 1636 (1955); $\underline{103}$, 862 (1966); J. Neufeld and W. S. Snyder, *ibid*. $\underline{99}$, 1326 (1955).

[46]G. Leibfried and O. S. Oen, J. Appl. Phys. $\underline{33}$, 2257 (1962).

[47]G. Leibfried, Nukleonik $\underline{1}$, 57 (1958); Ref. 27, pp. 153–156.

[48]C. Lehmann, Nukleonik $\underline{3}$, 1 (1961).

[49]P. Sigmund, Radiat. Eff. $\underline{1}$, 15 (1969).

[50]J. Lindhard, V. Nielsen, M. Scharff, and P. V. Thomson, Kgl. Danske Videnskab. Selskab, Mat.-Fys. Medd. $\underline{33}$, No. 10 (1963).

[51]D. G. Doran, discussion following Ref. 3a; D. G. Doran and R. A. Burnett, in Ref. 3b, p. 403.

[52]D. K. Holmes, in *The Interaction of Radiation with Solids*, edited by R. Strumane, J. Nihoul, R. Gevers, and S. Amelinckx (North-Holland, Amsterdam, 1964), p. 147.

[53]R. R. Coltman, C. E. Klabunde, and J. K. Redman, Phys. Rev. $\underline{156}$, 715 (1967).

[54]M. T. Robinson, in *Nuclear Fusion Reactors* (British Nuclear Energy Society, London, 1970), p. 364.

[55]R. B. Leachman, in *Proceedings of the First International Conference on Peaceful Uses Atomic Energy, Geneva*, 1955 (United Nations, New York, 1956), Vol. 2, p. 193.